Organic Process Research & Development **2009,** *13,* 276–279

Identifying Scale Sensitivity for API Crystallizations from Desupersaturation Measurements

Utpal K. Singh,* Mark A. Pietz, and Michael E. Kopach

Chemical Product Research and Development, Eli Lilly & Co., Inc. Indianapolis, Indiana 46285, U.S.A.

Abstract:

The present report details a methodology for discriminating between mass transfer- and surface integration-controlled crystallizations. Initial desupersaturation rates were measured, and a simple kinetic model was developed as a diagnostic tool for identifying scale sensitivity. The model was further extended to evaluate the impact of trace impurities on crystallization kinetics. Together, these results highlight the importance of understanding the factors that affect crystallization kinetics upon scale-up.

Introduction

The need to understand the active pharmaceutical ingredient (API) crystallization process is a fundamental part of the development of a physical property control strategy. One key aspect of this understanding relates to the measurement of crystallization kinetics and its exploitation for supersaturation control. The present report highlights development efforts toward obtaining reproducible scale-independent supersaturation control during crystallization of an API.

Unexpected buildup of supersaturation upon scale-up can have a deleterious effect on polymorph control and final API physical properties. In the case of a system with multiple polymorphs with small differences in solubility between the polymorphs, supersaturation control is necessary to obtain the desired polymorph in a reproducible manner.[1] Unexpected supersaturation buildup upon scale-up can also result in increased secondary nucleation and particle size distributions that may be different at pilot-plant scale compared to laboratory scale.

Scale sensitivity of supersaturation control can be attributed to several factors including changes in impurity load, mixing characteristics, and mass transfer rates across the particle boundary layer upon scale-up. Understanding the impact of these factors requires a detailed knowledge of crystallization kinetics which can be used to deconvolute mass transfer-limited processes from the surface integration-limited processes. In general, surface integration-limited processes would be expected to be scale independent, whereas mass transfer-limited processes would be expected to be highly scale dependent and affected by mixing and hydrodynamic conditions. Accurate measurement and modeling of crystallization kinetics can sometimes be an insurmountable challenge due to the complex steps involved. Braatz and co-worker[2] have utilized a powerful and mathematically rigorous methodology; however, this process can, at times, be mathematically intensive and difficult to implement.[2] The present report documents a case study in which the crystallization kinetics were measured using conventional desupersaturation techniques and modeled using simple growth and mass transfer models. The resulting temperature dependency of the desupersaturation rate (i.e., activation energy) and effect of mixing was used to identify conditions in which surface integration or mass transfer processes dominated. Karpinski and co-workers have conducted extensive investigations to determine rates of mass transfer and crystallization growth; however, the bulk of their work is focused on fluidized bed crystallizers and not stirred tank reactors as is the case in the present report.[3] Similar analysis is routinely conducted for multiphase reaction systems but is often neglected for industrial crystallization applications.

This technique was also useful in understanding the effect of impurities on crystallization kinetics. Trace levels of impurities suppressed the crystallization kinetics in the present system not only in the overall rate but also in the activation energy. Suppression of crystallization rates have been well documented;[4] however, the effect of impurities on activation energy and resulting impact on scale-up is seldom considered.

Experimental Procedure

Measurement of Crystallization Kinetics. The standard crystallization kinetics experiments were conducted on a 100-mL scale in a standard 125-mL jacketed three-neck round-bottom flask connected to a condenser and an overhead agitator and a 5-cm diameter half-moon crescent blade. Recrystallized (99.9%) API was dissolved in a known quantity of isobutanol (anhydrous, Aldrich) and water at elevated temperatures, i.e., 80−100 °C, prior to cooling to the desired temperature to obtain a supersaturated solution (20−30% supersaturation). The mixture was seeded with 1.5 m^2/g seed crystals (18 μm mean particle size). Periodic slurry samples were taken and immediately filtered using preheated Whatman AUTOVIAL Syringeless Filter and diluted with 1:1 acetonitrile/water and

* Author to whom correspondence may be sent. E-mail: singh_utpal@lilly.com.

(1) Jones, H. P.; Davey, R. J.; Cox, B. G. *J. Phys. Chem. B* **2005**, (109), 5273–5278.

(2) (a) Togkalidou, T.; Tung, H. H.; Sun, Y.; Andrews, A.; Braatz, R. D. *Ind. Eng. Chem. Res.* **2004**, (43), 6168–6181. (b) Matthews, H. B.; Rawlings, J. B. *AIChE J.* **1998**, (44), 1119–1127.

(3) (a) Karpinski, P. H. *Chem. Eng. Sci.* **1985**, (40), 641–646. (b) Karpinski, P. H. *Chem. Eng. Sci.* **1980**, (35), 2321–2324. (c) Budz, J.; Karpinski, P. H.; Nuruc, Z. *AIChE J.* **1985**, (31), 259–268.

(4) (a) Kitamura, M. *J. Cryst. Growth* **2002**, (237−239), 2205–2214. (b) Kitamura, M.; Ishizu, T. *J. Cryst. Growth* **1998**, (192), 225–235. (c) Berkovitch-Yellin, Z.; Mil, J. M.; Addadi, L.; Idelson, M.; Lahav, M.; Leiserowitz, L. *J. Am. Chem. Soc.* **1985**, (107), 3111–3122. (d) Sangwal, K. *Prog. Cryst. Growth Charact. Mater.* **1996**, *32* (1−3), 3–43.

10.1021/op8002344 CCC: $40.75
Published on Web 02/10/2009

analyzed by HPLC. The effect of temperature was measured by conducting the experiments at different temperatures and identical initial relative supersaturation. To that extent, the initial amount of API dissolved in isobutanol/water was varied, depending on the solubility. Additionally, the amount of seed charged in each experiment was varied to maintain constant seed loading with respect to the total quantity of API that was to crystallize.

Measurement of the Effect of Mass Transfer on Crystallization Kinetics. The effect of stirring speed was tested by conducting the kinetics studies using an IKA T-18 disperser with a S18N-19G dispersing element (12.7-mm rotor and 19-mm stator) as the agitation source in a jacketed 125-mL flask.

Effect of Impurities on Crystallization Kinetics. The effect of process impurities was evaluated by conducting the desupersaturation experiments using process mother liquors streams after the final reaction and subsequent workup. The streams had trace levels of impurities that were primarily inorganic salts and trace levels of structurally similar impurities all less than 0.1%. Additional kinetics studies were also conducted by dissolving ultrapure API in the presence of the impurities, i.e., the process stream.

Results and Discussion

In a growth-dominated regime, desupersaturation rates can be empirically described as follows:[5]

$$R_{\text{growth}} = k_g A \left(\frac{C_{\text{soln}} - C^*}{C^*} \right)^g \qquad (1)$$

where k_g, A, C_{soln}, C^*, and g are apparent crystallization rate constant, solid surface area, the solution concentration at a given time, solubility, and order in supersaturation, respectively. For the purposes of the present methodology, we have assumed surface integration is first order, i.e., $g = 1$. Our results cannot conclusively rule out a higher-order dependency of the growth rate on supersaturation. However, simulations using eq 1 (along with $g = 1$) and the measured rate constants from initial desupersaturation rate measurements adequately describe the crystallization system as evidenced by a reasonable agreement between the simulated and measured concentration profiles for a linear 2-h cool-down from 80 to 20 °C over 2 h as shown in Figure 1.[6]

Under mass-transfer controlling conditions, the apparent crystallization rate constant in eq 1 is the mass transfer constant for transport across the particle boundary layer which typically

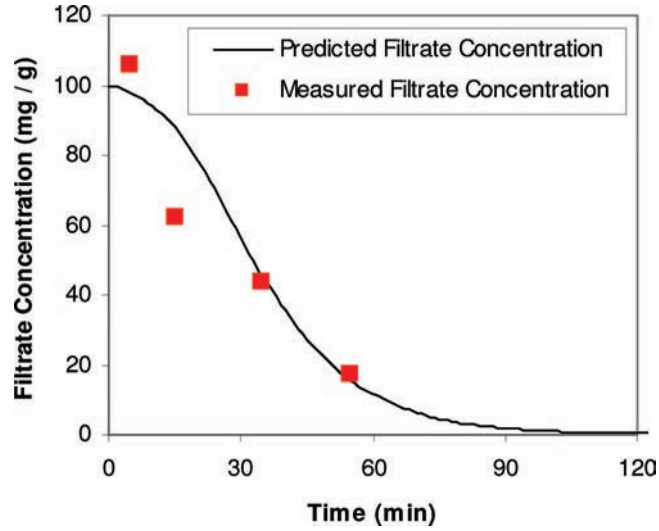

Figure 1. **Comparison of measured and simulated filtrate concentrations for a linear 2-h cool-down. The solid line was obtained through simulation of the crystallization process from initial desupersaturation rate measurements.**

exhibitd activation energies of 3−5 kcal/mol.[5,7] Under surface integration-controlled crystallizations, the apparent crystallization rate constant in eq 1 is the surface integration rate constant which typically exhibits activation energies of 10−15 kcal/mol.[5,7] As a result, the temperature dependency of the lumped rate constant k_g can be used to discriminate between mass transfer- and surface integration-controlled crystallization. These values have been documented in the literature for inorganic salts, and the present report suggests that similar trends appear to hold also for organic substrates.

The initial rate measurements from the desupersaturation studies are converted to a rate constant as follows:[8]

$$k_g = \frac{\left(\frac{dC_{\text{soln}}}{dt} \right)_{t=0} M_{\text{mix}}}{A^0_{\text{seed}}} \qquad (2)$$

where A_{seed}, M_{mix}, and dC_{soln}/dt are the initial seed surface area, mass of the crystallization mixture, and initial slope, respectively. The initial rates were measured by calculating the slope from desupersaturation of the initial 30% of the overall supersaturation consistent with conventional differential kinetics treatment.

Desupersaturation kinetics with 3 vol % water in isobutanol were measured between 20 to 60 °C, and an activation energy

(5) Garside, J., Mersmann, A., Nyvlt, J., *Measurement of Crystal Growth and Nucleation Rates*, 2nd ed.; Institution of Chemical Engineers: U.K., 2002; p 18.

(6) The simulated concentration profile, for a given set of rate constants, activation energy, and temperature profile, was obtained by numerically solving the differential equation resulting from the instantaneous mass balance at a given time: $dM/dt = -k^*A^*dC/C^*$ where M, k, A, and dC/C^* are the mass of solute in solution, rate constant of desupersaturation, area of crystallized API, and the relative supersaturation, respectively. The area was assumed to change in a self-similar manner as follows: $A = A^0{}^*(M/M^0)$ (2/3) where A^0, M^0, M are the initial seed surface area, initial seed mass, and mass of API out of solution at a given time.

(7) Mullin, G. W. *Crystallization* 3rd ed.; Butterworth-Heinemann: Boston, 2000.

(8) For the rate formulation in eq 1, the pseudo-first-order rate constant can be expressed as:

$$k_g = \frac{\left(\frac{dC_{\text{soln}}}{dt} \right)_{t=0} M_{\text{mix}}}{A^0_{\text{seed}} \left(\frac{C - C^*}{C^*} \right)^{g-1}}$$

For the case of $g = 1$, this expression collapses to that shown in eq 2.

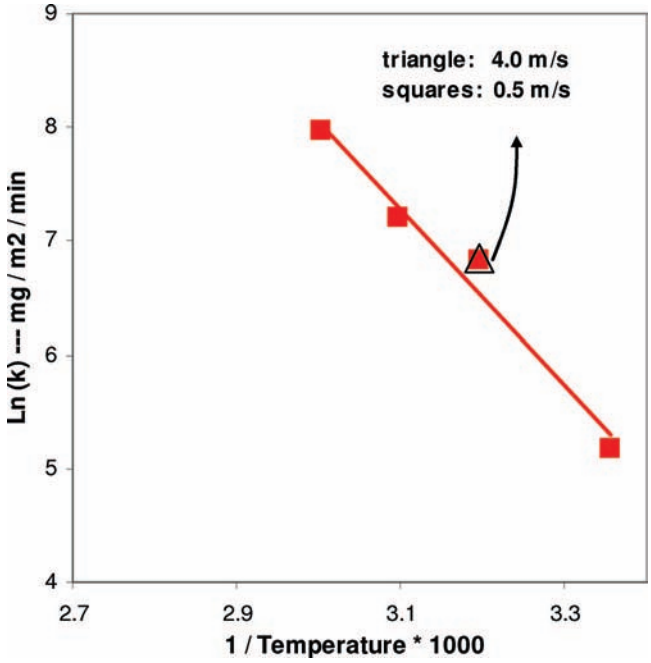

Figure 2. **Arrhenius plot for the crystallization of API in isobutanol with 3% water.**

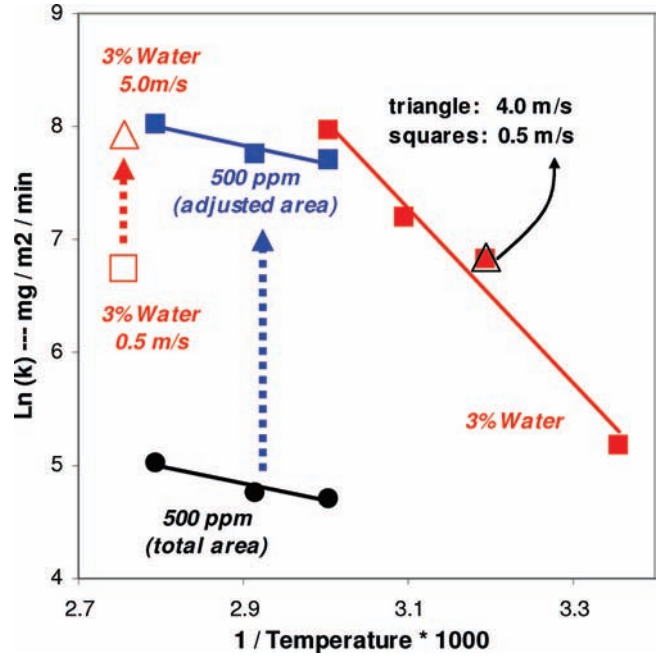

Figure 3. **Arrhenius plot for the desupersaturation of API in isobutanol at varying levels of water and agitation speed.**

of 15 kcal/mol was observed, assuming Arrhenius-type relationship (See Figure 2-red filled squares). A repeat of the 40 °C experiment in Figure 1 using a high-speed IKA disperser with an 8-fold increase in tip speed resulted in vigorous mixing; however, the rate constant for desupersaturation was unaffected (Figure 1-black unfilled triangle), further reinforcing the hypothesis that the crystallization is not mass transfer limited, but rather surface integration limited under these conditions.

The absence of significant nucleation effects during the desupersaturation experiments could not be ruled out conclusively; however, the final particle size at the completion of the desupersaturation experiments were in agreement with expectations from a model assuming two- or three-dimensional self-similar growth.[9] Specifically, 50−100 μm particles present in the seed compared to approximately 100−200 μm particles upon completion of the desupersaturation experiment with 7.4% seed. Additionally, the initial rate of desupersaturation and final particle size, measured by microscopy, at 70 °C and 70% supersaturation were similar to those observed at 70 °C and 26% supersaturation.

Impact of Mass Transfer Resistance on Crystallization Kinetics. Extrapolation of the Arrhenius rate law in Figure 1 to 90 °C predicts a desupersaturation rate of 20,700 mg/m^2/min compared to a measured value of 840 mg/m^2/min (open red square in Figure 3), indicating a significant change in the activation energy at temperatures greater than 60 °C. The conditions required to measure desupersaturation rates at 90 °C required a 25 wt % solution which was significantly more viscous than the 5−7 wt % solutions that were utilized in the standard desupersaturation conditions resulting in a poorer mass transfer conditions. A repeat of the 90 °C experiment under more vigorous mixing conditions using an IKA high-speed disperser at 5 m/s tip speed resulted in 3-fold increase in the measured rate to 2771 mg/m^2/min (open red triangle in Figure 2) consistent with a mass transfer-limited process. This stands in stark contrast with results at 40 °C in which a 8-fold increased tip speed had no effect on the initial desupersaturation rates (open triangles and filled red squares in Figure 3).

The increase in the desupersaturation rate at 90 °C with an increase in tip speed cannot be attributed to secondary nucleation effects alone since the desupersaturation kinetics at 40 °C was unaffected by a similar increase in tip speed (using identical seed source and supersaturation). Additionally, the seed had been pin milled, resulting in micronized 18 μm particles, and it is unlikely that the IKA disperser would result in further reduction in particle size. Therefore, further attrition or secondary nucleation effects alone are considered unlikely to be the source of the increased desupersaturation rate with increased mixing intensity using the IKA T-18 disperser.

Conducting the desupersaturation experiments at higher temperatures, i.e., greater than 60 °C, and using lower water concentrations (500 ppm) resulted in a lower measured growth rate and an activation energy of 3 kcal/mol (Figure 3-filled black circles). No differences in polymorphs were observed; however on average, thinner, more needlelike morphology was observed with 500 ppm water in contrast with the 3% water system. This morphology effect was further accentuated by repeated thermal cycling that yielded larger, thicker rods in the presence of 3−5% water. On the basis of these observations, the desupersaturation rates measured under low water conditions were normalized to

(9) Fraction seed load = (mass of added seed)/(final mass after crystallization including seed). For a given size, constant shape factor for seed and final particles, and constant crystal density, this collapses to: Fraction seed load = (radius of seed particle)^3/(radius of final particle size)^3.

(10) Total surface area of a rod with a length and width of l and d, respectively is: $2*d^2 + 4*d*l$. The surface area of the edge of the rods is $2*d^2$. The ratio of the total surface area of entire rod to the surface area of small faces of the rod is approximately 2*AR where AR is the aspect ratio of the rod, i.e., l/d (ratio of length of the rod to the width of the rod). Image analysis yielded an aspect ratio of approximately 10:1.

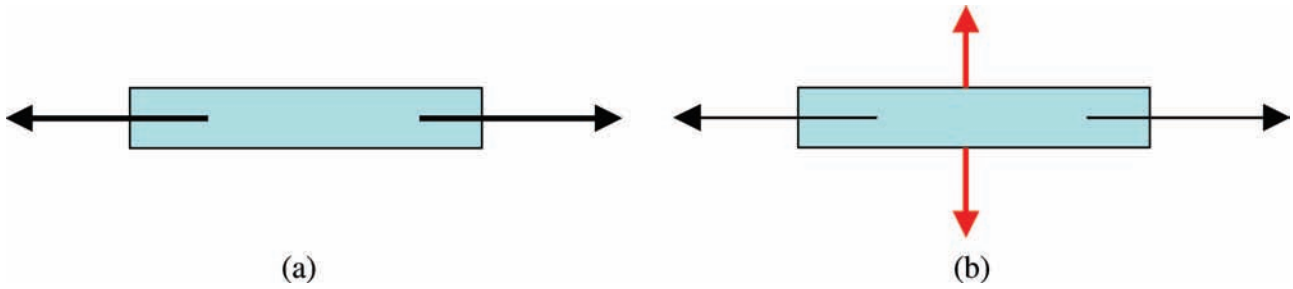

Figure 4. **Impact of water content on the surfaces available for growth: (a) anhydrous in isobutanol and (b) 3% water in isobutanol.**

the available surface area for growth, i.e., small faces of rods as shown in Figure 4 using the average aspect ratio.[10] The area-adjusted rates are plotted in Figure 3 (filled blue squares), and the trends indicate that the area-adjusted values are consistent with the measured mass transfer-limited rates (open triangles) as well as with the maximum rate observed with the 3% water system (filled red squares), suggesting a mass transfer-limited process under low water levels.

For the case of the API reported above, a simple kinetics model was effective in discriminating between surface integration-limited and diffusion-limited models. However, the generality of this model to other systems with greater tendency to nucleate is unclear and is the subject of further investigation.

Effect of Impurities on Crystallization Kinetics. The above section discriminated between mass transfer- and surface integration-controlled regimes; as a result, the effect of impurities on crystallization kinetics can be studied without the convolution of mass transfer effects. Desupersaturation rate measurements using in-process solution in the presence of trace levels (less than 0.2 area % impurities) of inorganic and structurally similar impurities resulted in an activation energy of 3 kcal/mol (filled triangles in Figure 5) compared to 15 kcal/mol for the 3% water system in an ultrapure recrystallized API. The lower activation energy in a region where mass transfer limitations are not controlling was also observed when the desupersaturation measurements were conducted with ultrapure API using mother liquors containing process impurities (open squares in Figure 5), further confirming the role of impurities in decreasing the activation energy.

There are several mechanisms or combination of mechanisms that may be at play in the impurities affecting the activation energy,[4,11] and determining the exact inhibition mechanism is outside the scope of the present work. Additional modeling efforts are necessary to determine the dominant mechanism at play. However, regardless of the mechanism by which the impurities affect the crystallization kinetics, the results highlight an often overlooked fact with industrial crystallizations: that trace levels of impurities not only impact solubility and rate but also significantly affect the activation energy which can in turn affect supersaturation control upon scale-up. There may be cases in which fast diffusion limited-crystallization processes become surface integration-limited due to impurity poisoning of the crystal surface. Understanding such a transition would be important since enhanced

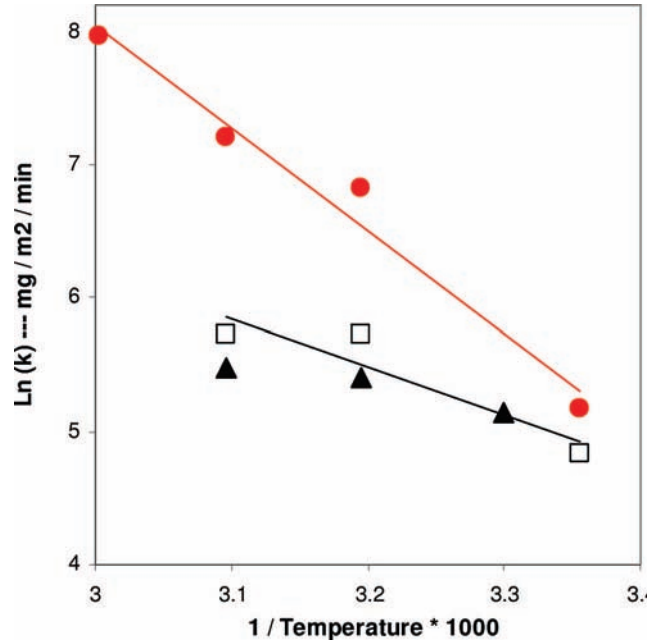

Figure 5. **Arrhenius plot showing a comparison of the desupersaturation kinetics using (a) ultrapure API in clean solvent [red circles], (b) process stream containing trace levels of impurities [filled triangles]; (c) ultrapure recrystallized API in process mother liquors [open squares].**

mixing characteristics are unlikely to impact the crystallization rate. Process optimization during the course of a process development routinely results in changes in impurity content; and as a result, subsequent crystallization and scale-up efforts should be conducted by understanding its effect on crystallization kinetics. Further efforts are underway to determine the generality of the phenomenon described above.

Conclusions

The results highlight the use of simple desupersaturation kinetics as a diagnostic tool for determining scale sensitivity of a crystallization. The present report highlights the use of activation energy to discriminate between mass transfer- and surface integration-controlled crystallizations as well as the effect of trace levels of structurally similar impurities. The generality of this phenomenon is under further investigation.

Received for review September 20, 2008.

OP8002344

(11) Martins, P. M.; Rocha, F. A.; Rein, P. *Cryst. Growth Des.* **2006**, *6* (12), 2814–2821.